

## How can slow plasma electron holes exist?

I. H. Hutchinson *Plasma Science and Fusion Center, Massachusetts Institute of Technology, Cambridge, Massachusetts 02139, USA*

(Received 28 April 2021; accepted 21 June 2021; published 15 July 2021)

One-dimensional analysis is presented of solitary positive potential plasma structures whose velocity lies within the range of ion distribution velocities that are strongly populated: “slow” electron holes. It is shown that to avoid the self-acceleration of the hole velocity away from ion velocities it must lie within a local minimum in the ion velocity distribution. Quantitative criteria for the existence of stable equilibria are obtained. The background ion distributions required are generally stable to ion-ion modes unless the electron temperature is much higher than the ion temperature. Since slow positive potential solitons are shown not to be possible without a significant contribution from trapped electrons, it seems highly likely that such observed slow potential structures are indeed electron holes.

DOI: [10.1103/PhysRevE.104.015208](https://doi.org/10.1103/PhysRevE.104.015208)

### I. INTRODUCTION

Solitary positive potential structures are observed by satellites in some space plasmas to have speeds comparable to the typical ion thermal speed, even lying within the strongly populated velocities of the ion distribution [1–3]; that is what is meant here by calling the structures “slow.” A candidate explanation of these structures is that they are “slow electron holes,” in which the positive potential is sustained by a deficit of trapped electrons. However, until now it has been unclear theoretically whether, or under what circumstances, slow electron holes can exist. The purpose of the present study is to discover the theoretical conditions for the existence of plasma-sustained steady slow solitary positive potential structures, including electron holes, and identify the mechanisms that control them. Figure 1 shows contours of electron and ion velocity distribution functions  $f(v)$ , for a presumed steady slow potential peak, in their respective  $x, v$  phase spaces (using conveniently normalized units). For *trapped* electron orbits,  $f_e(v)$  is determined by conditions during the structure’s formation and has lower value than the nearby passing orbits which are determined by the boundary conditions. This results in a more negative central electron density than ion density and causes the potential peak. (Electron contour values are not important to this illustrative discussion and not shown.) The ion distribution is everywhere determined by the distant distribution function and the fact (arising from Vlasov’s equation) that  $f$  is constant along orbits. Orbits have constant energy for a steady potential. Ions are reflected by the hole if their speed in the hole frame is small enough. The illustrative case shown corresponds to Maxwellian ion distribution at large  $|x|$ , with zero average velocity in the hole frame. That is, this hole has zero velocity in the ion frame.

The reasons to question whether slow electron holes can exist are to do with the interaction of their positive potential peak with the ions. Classic electron holes move at speeds, relative to ions, up to of order the electron thermal speed  $v_{te}$  [4,5]. And when they are at more than a very small fraction

of  $v_{te}$ , the ion perturbation is small because the duration of any moving electron hole’s interaction with an ion is much smaller than the typical response time of the (far heavier) ions. Ion response can then often be completely ignored. As has been extensively discussed, for example in the original paper on BGK modes [6] and the electron hole review literature [5] the detailed shape of the hole has considerable latitude to adjust itself to the details of the trapped electron velocity distribution, and is only a minor consideration here, limiting the discussion to potentials with a single maximum.

For slower holes, ion interaction gradually becomes important. When hole speed is less than a few [up to about  $(m_i/m_e)^{1/4}$ ] times the ion acoustic speed ( $c_s = \sqrt{T_e/m_i}$ ), the ion interaction is significant, and the electron hole speed resists approaching the ion speed [7,8], maintaining a velocity (difference) greater than a minimum that increases with hole potential. If the hole speed is less than that minimum, then an oscillatory instability in the hole speed arises [9] and there is therefore a forbidden region of hole speed. This forbidden velocity region has a lower limit that is at approximately the ion-acoustic soliton speed, which is just above  $c_s$  (depending on peak potential [10]). At that specific speed, an entity usually called a coupled hole-soliton (CHS) is known from simulations [11–13] to exist. In effect the electron hole is trapped in, and enhances, the positive potential produced at that speed by the positive ion density perturbation of the ion-acoustic soliton. A CHS generally moves faster than the ion thermal speed, provided the electron temperature is greater than ion temperature, so there are few ions in the distribution at the CHS speed, and Landau damping can be small.

It is emphasized that none these known types of theoretical holes qualifies for the present meaning of “slow.” Neither do holes produced by the Bunemann instability when there is substantial drift between ion and electron populations, invoked by Norgren *et al.* [14,15] to explain their space observations. Holes produced [13,16,17] by Bunemann instability usually have speeds (relative to ions)  $\ll v_{te}$  but not  $< c_s \simeq \sqrt{m_e/m_i} v_{te}$  let alone  $\sim v_{ti}$ . Instead, the present paper

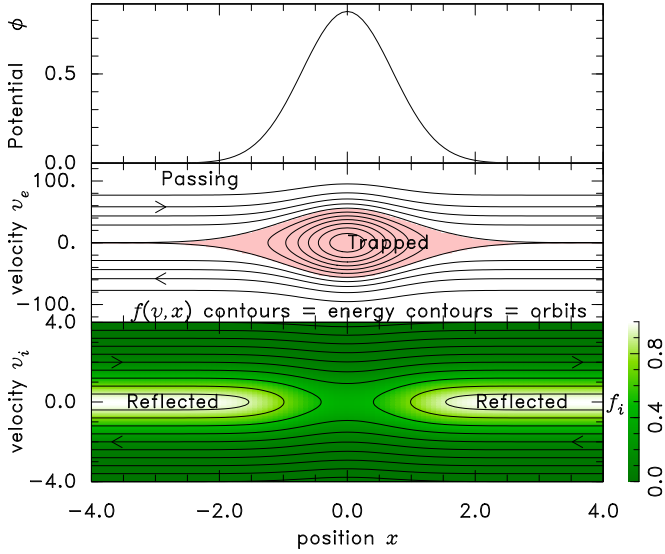


FIG. 1. Schematic of a slow electron hole and the corresponding electron and ion phase-space density contours.

addresses the “Group 3” electron holes observed by Steinvall *et al.* [2] (“on the magnetospheric side of the magnetopause”) that have speeds relative to ions below  $c_s$  (Group 1 speeds exceed the oscillatory instability threshold, and Group 2 are consistent with being CHS type). A fraction of the observations of Graham *et al.* [1] (“near the magnetopause”) and of the blue points in Fig. 4 of Lotekar *et al.* [3] (magnetotail) also are slow in the present sense.

Simulations that initialize an electron hole at speeds of order the ion thermal speed  $v_{ti}$  or less in an initially uniform ion background, observe a remarkable and rapid “self-acceleration” of the hole [8,11,18–20]. The growing negative ion density (and hence charge) perturbation caused by the repulsion of ions from the positive potential of the hole repels the electron hole, because an electron hole’s dynamics as a composite entity are such that it has an effective charge to mass ratio equal to that of the electron [7,21]. A short time after initialization, it moves away at speeds much larger than  $v_{ti}$ . Thus, past simulation attempts have failed to produce steady slow electron holes.

The novelty and complexity of the present analysis in comparison with the prior treatments of ion-acoustic solitons and electron holes is that it *requires a kinetic* (rather than fluid, e.g., Ref. [22]) treatment of the ions in equilibrium. Concerning past kinetic electron hole analysis (e.g., Ref. [23]) and simulations (e.g., Ref. [19]), the key difference is that the present analysis shows that for *slow* positive structures to exist stably, the background ion velocity distribution generally cannot be “single-humped.” It must instead possess at least two maxima. Indeed, it is shown that slow positive solitary potentials sustained by trapped electron deficit (1) cannot persist in single-humped ion distributions, (2) can persist only when the velocity of the electron hole lies within a local minimum of the ion distribution function, but (3) do not require background distributions that are ion-ion unstable, provided the electron temperature is not very high. All the discussion here is one-dimensional, and multidimensional stability is beyond

the present scope. The conclusion therefore is that, from a one-dimensional perspective, slow electron holes can exist, requiring distinctively nonthermal external ion distributions; but those distributions are not themselves unstable and can therefore persist for substantial time durations.

These theoretical characteristics are valuable for identifying the nature of slow solitary potential peaks observed in plasmas, and for indicating the presence of double-humped ion distributions. Recent analysis reported elsewhere Ref. [24] of satellite measurements confirm the characteristics for slow electron holes observed in the plasma sheet boundary layer.

Section II addresses ion distribution functions that have reflectional symmetry in some reference frame. The simplifications of symmetry make it easier to understand the concepts introduced and permit straightforward proofs concerning stability and equilibrium. Section III generalizes these results to asymmetric ion distributions, and Sec. IV addresses the question of the linear stability of the uniform background ion distributions found to be necessary for the existence of slow electron holes.

## II. SYMMETRIC DISTRIBUTION FUNCTIONS

Consider a steady solitary positive potential structure in one dimension:  $\phi(x)$ , possessing a single maximum  $\phi = \psi$  at position  $x = 0$ , and tending to the same potential  $\phi = \phi_\infty = 0$  at distant positions  $x \rightarrow \pm\infty$ . For motion in this single dimension, suppose the distribution function of ions approaching the potential structure from the distant plasma to be given as  $f_\infty(v_\infty)$ , in a frame of reference in which the structure is stationary.

A collisionless ion equilibrium satisfies the steady Vlasov equation, giving conservation of distribution function and energy on orbits, leading to

$$f(x, v) = f_\infty(\infty, v_\infty) \quad \text{where} \quad v^2/2 + \phi(x) = v_\infty^2/2 + \phi_\infty. \quad (1)$$

In this paper, to abbreviate the equations we mostly work in conveniently scaled units: energy normalized to thermal energy for a reference temperature  $T_0$ , length normalized to Debye length  $\lambda_D = \sqrt{\epsilon_0 T_0 / e^2 n}$ , and velocity to ion thermal speed  $\sqrt{T_0 / m_i}$ . In these units, the ion mass and charge are unity. Where numerical values of quantities like distribution function, density, or force-density, etc., are presented, they are for unit background density  $n_\infty$ .

When the ion distribution function *in the rest frame of the structure* is not symmetric, very substantial analytic complications nevertheless arise from ion reflections. We shall address these in a subsequent section, but initially it is simpler to exclude those complications by assuming the distribution to be reflectionally symmetric in ion velocity  $v$ .

### A. Single-humped distributions: Density in equilibrium

Since  $f_\infty(v_\infty)$  is symmetric in the sign of  $v_\infty$ , using  $vdv = v_\infty dv_\infty$  one can simply write the (ion) density as

$$n = 2 \int_{|v_\phi|}^{\infty} f_\infty \frac{v_\infty dv_\infty}{\sqrt{v_\infty^2 - v_\phi^2}} = -2 \int_{|v_\phi|}^{\infty} f'_\infty \sqrt{v_\infty^2 - v_\phi^2} dv_\infty, \quad (2)$$

where  $|v_\phi| = \sqrt{2(\phi - \phi_\infty)}$  is the speed at infinity of ions that are reflected at the position  $x$  and potential  $\phi$  and prime denotes differentiation with respect to argument ( $v_\infty$ ). This density is then simply a function of  $\phi$ . Express the density far from the potential structure as

$$n_\infty = 2 \int_0^\infty f_\infty dv_\infty = -2 \int_0^\infty f'_\infty v_\infty dv_\infty, \quad (3)$$

and so deduce the density change introduced by the presence of the potential structure:

$$n - n_\infty = 2 \int_0^{|v_\phi|} f'_\infty v_\infty dv_\infty + 2 \int_{|v_\phi|}^\infty f'_\infty [v_\infty - \sqrt{v_\infty^2 - v_\phi^2}] dv_\infty. \quad (4)$$

When  $f_\infty$  has only a single maximum (at  $v = 0$ )  $f'_\infty$  is negative throughout the integrals. The functions multiplying  $f'_\infty$  in the integrands are everywhere positive; so for symmetric single-humped  $f_\infty$ , we have  $n < n_\infty$ : The ion density change arising from a positive potential is always negative. This is one indication that a positive potential soliton sustained by ions cannot exist at low speed relative to the ion thermal (or acoustic) speed. The density perturbation has the wrong polarity for self sustainment. What is more, as we shall see in the next section, this observation has important consequences for the possibility of slow electron holes. For single-humped  $f_\infty$  they will have negative ion charge relative to the external plasma. This negative ion charge repels the electron hole that causes them. The result is rapid acceleration of the electron hole until it has speed higher than typical ion thermal speeds. Such unstable acceleration has been well documented in simulations [8,19,25]. Thus the slow electron hole equilibrium in a single-humped ion distribution is unstable to hole acceleration.

### B. Force and acceleration of the potential structure

To make a more quantitative assessment of slow hole dynamics, it is simplest to find the total force exerted on the ions by the entire potential profile  $\phi(x)$  (per unit area perpendicular to  $x$ ). Evidently, it is  $F = \int \rho E dx = - \int_{-\infty}^\infty n(x) \frac{d\phi}{dx} dx = - \int n(\phi) d\phi$ . When  $f_\infty$  is symmetric,  $n(\phi)$  is independent of the sign of  $x$ , denoted  $\sigma_x$ , while  $d\phi/dx$  has sign  $-\sigma_x$ . Therefore, in steady state regardless of the shape of  $\phi(x)$ , the total force on the ions is zero, as a consequence of symmetry. Perhaps more significantly, the reaction force exerted by the ions on the potential structure ( $-F$ ) is also zero. It is in equilibrium.

Suppose, however, that the potential structure is stationary  $\phi_0(x)$  (in the equilibrium frame) and remains in steady equilibrium long enough for the ion density to reach the value given by Eq. (2); but then some perturbative uniform displacement  $\delta x$  of the potential structure (in the equilibrium frame) begins, which is rapid relative to the timescale of adjustment of the ion density to the movement. This presumption is a good approximation for an electron hole experiencing unstable acceleration as has been shown analytically [7], and by simulation [8] elsewhere. Also, the timescale for electron motion and hence structure motion is much shorter (by

$\sim \sqrt{m_e/m_i}$ ) than for ion motion. After a short time, the density of the slowly responding ions,  $n(x)$ , will to lowest order be unchanged, it remains a function of the steady potential  $\phi_0$ , but will no longer be a function of the instantaneous potential  $\phi = \phi_0 + \delta\phi$ . Consequently the symmetry is broken, and total force on the ions will be nonzero. The linearized perturbation for a small rigid shift  $\delta x$  of the potential structure [27] is  $\delta\phi \approx -\frac{d\phi_0}{dx} \delta x$  which is antisymmetric. The ion force increment is

$$\begin{aligned} \delta F &= - \int n(x) \frac{d\delta\phi}{dx} dx = \delta x \int n(x) \frac{d^2\phi_0}{dx^2} dx \\ &= -\delta x \int \frac{dn}{dx} \frac{d\phi_0}{dx} dx = -\delta x \int \frac{dn}{d\phi_0} \left( \frac{d\phi_0}{dx} \right)^2 dx. \end{aligned} \quad (5)$$

Now the potential structure has been displaced from equilibrium and experiences a force  $-\delta F = -C\delta x$ , where the coefficient is  $C = \delta F/\delta x = - \int \frac{dn}{d\phi_0} \left( \frac{d\phi_0}{dx} \right)^2 dx$ . Incidentally, this force is related to imbalanced reflection of the ions from the potential structure and ion jetting. Imbalanced reflection of electrons from small negative-potential *ion holes* is proportional to the slope of the electron distribution function at the hole speed [28]. But for positive structures it is better to express the force in terms of these instantaneous integrals, since full reflection of ions takes much longer to transfer their momentum to the structure than the timescale of hole motion. Whether or not the structure regarded as a rigid composite object continues to be displaced or returns to its equilibrium position depends on the sign of its acceleration, and hence on the sign of  $C$ , which is evidently minus the sign of  $dn/d\phi_0$  (averaged over the hole with positive definite weight); but it also depends on the structure's response to force, that is, its effective mass  $M$ .

Supposing the potential structure to be an electron hole, one can deduce the acceleration of the hole by requiring the total of electron ( $\dot{P}_e$ ) and ion ( $\dot{P}_i$ ) momentum rates of change to be zero (since the electric field momentum is negligible):  $0 = \dot{P}_i + \dot{P}_e = \delta F + \dot{P}_e$ . Thus the effective mass of the hole, its force divided by acceleration, is  $M = -\delta F/\delta\ddot{x} = \dot{P}_e/\delta\ddot{x}$ . The electron momentum change arises from jetting by the accelerating potential structure, and is given by Eq. (34) of Ref. [7] in dimensional units

$$\dot{P}_e = -\delta\ddot{x} n_e m_e \int h(\chi) dx, \quad (6)$$

where  $h(\chi)$  is a non-negative function [29] of argument  $\chi \equiv \sqrt{|e\phi|/T_e}$ . For negligibly shifted Maxwellian electrons  $h$  can be written in closed form as

$$h(\chi) = -\frac{2}{\pi} \chi + [(2\chi^2 - 1)e^{\chi^2} \text{erfc}(\chi) + 1]. \quad (7)$$

The effective electron hole mass (per unit transverse area)  $M = -n_e m_e \int h(\chi) dx$  is thus negative.

Within the present lumped approximation, the equation of motion of the potential structure is  $\delta\ddot{x} = -(C/M)\delta x$ , giving eigenfrequency  $\omega = \pm\sqrt{C/M}$ . The *stability* of the initial symmetric equilibrium depends on the sign of  $C/M$ . Stable oscillation is expected for  $C/M$  positive, exponential growth for  $C/M$  negative. When ion density is decreased by positive potential,  $dn/d\phi_0 < 0$ ,  $C$  is positive. Therefore  $C/M$  is negative and the hole is unstable to displacements relative to the

equilibrium position and velocity when ion density change caused by positive potential is negative, as it is for symmetric single-humped ion distribution function.

The mass of a hole of small  $\psi$  can be calculated using the approximation  $h(\chi) \rightarrow \chi^2 = \phi T_0/T_e$  so in dimensional units  $M = -(n_e m_e/T_e) \int e \phi dx$ , and

$$\frac{C}{M} = \frac{-e \int \frac{dn}{d\phi_0} \left(\frac{d\phi_0}{dx}\right)^2 dx}{-(n_e m_e/T_e) \int \phi dx}. \quad (8)$$

Now we convert  $\phi$ ,  $\psi$ ,  $x$ , and  $C/M$  into dimensionless units dividing them by  $T_0/e$ ,  $\lambda_D$ , and  $\omega_{pi}^2$  respectively, and defining an effective dimensionless hole length  $L \equiv \int \phi dx/\psi$ . This yields the dimensionless form

$$\frac{C}{M} = \frac{-e \int \frac{dn}{d\phi_0} \left(\frac{d\phi_0}{dx}\right)^2 dx}{-(n_e m_e/T_e) \int \phi dx} \frac{1}{\lambda_D^2 \omega_{pi}^2} \simeq -2 \frac{T_e}{T_0} \frac{m_i}{m_e} \frac{\psi}{L^2}, \quad (9)$$

where, anticipating a result to be shown in Sec. II C, the dimensionless magnitude of the numerator for hole form  $\psi \text{sech}^4(x/\ell)$  and unit density Maxwellian ions is found to be approximately  $C = 2\psi^2/L$ . A self-consistent small-amplitude electron hole of the  $\text{sech}^4$  form has length  $L = (16/3)\lambda_{De} = (16/3)\sqrt{T_e/T_0}$  (dimensionless). Therefore  $C/M = -(3/16)^2 2\psi(m_i/m_e)$  and the growth rate is  $\gamma = \sqrt{2\psi m_i/m_e} (3/16)$  in  $\omega_{pi}$  units. It is perhaps more intuitive to write dimensionally

$$\gamma \simeq \frac{3}{16} \sqrt{\frac{2e\psi}{T_0}} \omega_{pe}. \quad (10)$$

This confirms that the instability is fast because it is on the electron timescale  $\omega_{pe}^{-1}$  rather than the ion timescale, hence justifying the model taking stationary ions during the motion of the potential structure. But if  $\psi$  is very small, then the gap between the reduced  $\gamma$  and the ion response time will eventually disappear, and the approximation become inadequate.

### C. Non-single-humped distribution function hole stability

For a stable electron hole or other positive potential structure attributable to the plasma itself to exist, we require the ion density perturbation that it produces to be non-negative. This is achieved in classic ion-acoustic solitons by the relative speed of the soliton and the ions being substantially larger than the ion thermal speed. A classic soliton is not slow in the current sense; and also the ion velocity distribution is not symmetric (in the structure frame) but consists of a single Maxwellian shifted by velocity  $v_b$ . Pursuing in this section only symmetric distributions, one can clearly make the distribution symmetric by introducing a symmetric second ion population of shift  $-v_b$ . In that case a soliton can exist, but physically it is still not “slow” in the sense of the structure velocity coinciding with the dominant part of the ion distribution.

This two-beam soliton situation shows qualitatively how to obtain positive ion density perturbation. Ions that are not reflected, because their energy exceeds the peak potential, contribute positively to the ion density perturbation because their speed  $|v|$  at positive potential is lower than at  $\phi_\infty$  (conserving energy) yet their flux ( $nv$ ) must be in-

dependent of position; so  $n$  must increase to compensate. A passing monoenergetic beam of ions has density  $n(\phi) = n_\infty v_\infty / \sqrt{v_\infty^2 + 2(\phi - \phi_\infty)}$ , which increases without bound near the potential  $\phi = \phi_\infty + v_\infty^2/2$  needed for reflection. Therefore, if the unreflected (passing) ion population is sufficiently dominant, then the ion density change is positive. What the previous subsection showed is that for *single-humped* symmetric distributions the passing population is never sufficiently dominant. A sufficiently widely spaced two-beam distribution can, however, achieve sufficient dominance. If the spacing  $2|v_b|$  is reduced, then eventually that dominance will be lost and the unstable negative ion density change  $[n - n_\infty]$  will reappear. The intuitive question therefore is quantitatively how small can the beam spacing be and still avoid instability. We already know from the previous subsection that part of the answer is that the distribution must be non-single-humped; in other words that it must have a local minimum. But how deep must the minimum be?

The stability threshold is determined, on the basis of the lumped treatment of electron-sustained structure motion, by the change of sign of the force coefficient,  $C = \delta F/\delta x = -\int \frac{dn}{dx} \frac{d\phi_0}{dx} dx = -\int \frac{dn}{d\phi_0} \left(\frac{d\phi_0}{dx}\right)^2 dx$ . Instability arises if  $\delta F/\delta x$  is positive. Its value is determined by both the distribution function [giving  $n(\phi_0)$ ] and potential profile  $\phi_0(x)$  (giving  $\frac{d\phi_0}{dx}$ ). However, its sign depends only on the relative shape of  $\phi_0(x)$ , not on its extent, because expanding or contracting the profile in  $x$  by a uniform (positive) scale factor  $\ell$  simply divides  $\delta F/\delta x$  by  $\ell$ . Thus, for example, a Gaussian potential  $\phi = \psi e^{-x^2/\ell^2}$  will give a very slightly different threshold than  $\phi(x) = \psi \text{sech}^4(x/\ell)$ , but neither threshold depends on the value of  $\ell$ . We choose  $\ell$  conveniently so as to make  $L \equiv \int \phi dx/\psi = 1$ , requiring  $\ell = 3/4$  for the  $\text{sech}^4(x/\ell)$  shape, in the following plots. Using instead a Gaussian with  $\ell = 1/\sqrt{\pi}$  gives plots that appear so similar they are not worth including. To an excellent approximation only the overall width  $L$  and height  $\psi$  of the hole control the quantitative values.

To evaluate  $\delta F/\delta x$  (numerically) for a specified distribution and potential shape, we must obtain  $n(\phi)$  by integrating Eq. (2) with respect to  $v_\infty$  and then integrate  $\int \frac{dn}{dx} \frac{d\phi_0}{dx} dx$  with respect to  $x$ , for the chosen shape  $\phi(x)$ . A code has been written to perform these integrations for arbitrary (input)  $f_\infty$  or for distributions consisting of multiple shifted Maxwellian components where their separation (and hence the depth of the local minimum) is scanned. For distributions consisting of two symmetric Maxwellian components of temperature  $T = T_0 = 1$ , shifted from  $v = 0$  by  $\pm v_b$ , Fig. 2(a) shows ion distribution shapes as  $v_b$  is varied, with the marginally stable cases for  $\psi = 0.02$  and  $\psi = 0.5$  emphasized in bold black and red. Figure 2(b) shows the force coefficients  $\delta F/\delta x/\psi^2$  (using  $L = 1$ ) as a function of beam shift  $v_b$  for a range of potential heights  $\psi$ . The magnitude of  $\delta F/\delta x$  scales approximately like  $\psi^2$  but because of nonlinearities in  $n(\phi)$  there is a small variation in the force and threshold with potential peak height.

As shown in Fig. 2(b), over a wide range of potential heights  $\psi$  the threshold  $v_b$ , where  $\delta F/\delta x$  crosses zero, varies a modest amount (between 1.3 and 1.5), and the corresponding depth of the minimum  $(f_{\max} - f_{\min})/f_{\max}$  is a fraction of the  $f$ -maximum that lies between 0.20 and 0.36. Greater  $\psi$  requires deeper minimum.



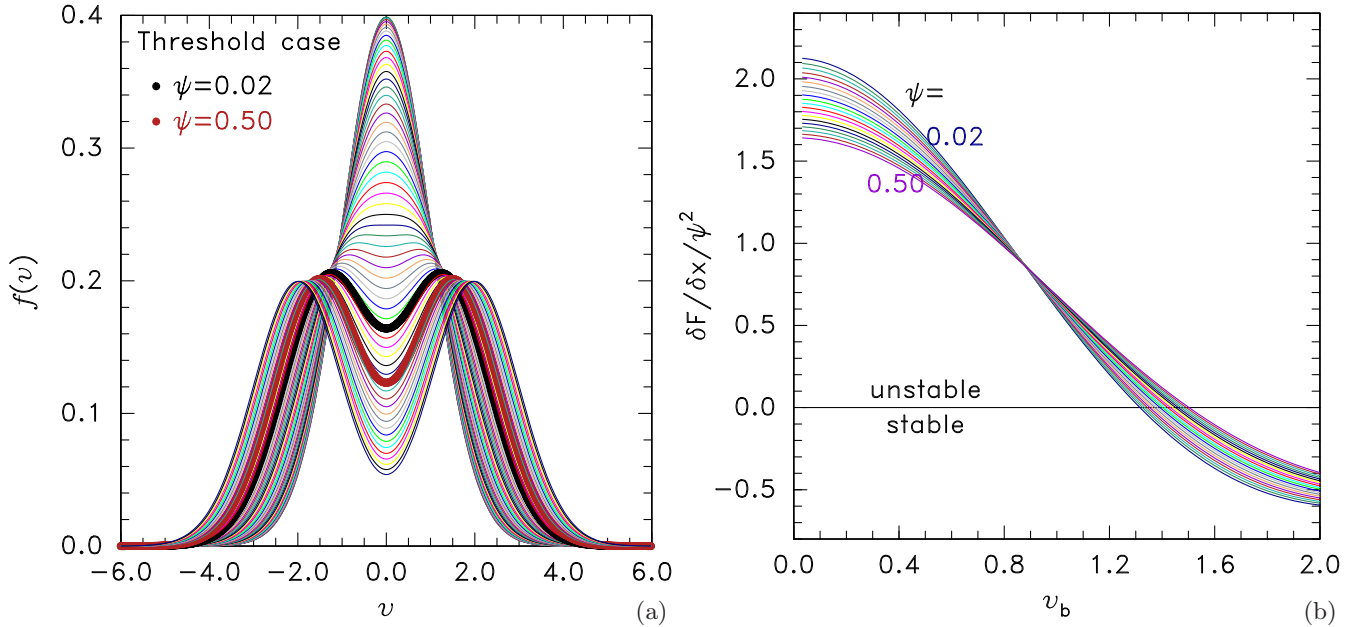


FIG. 2. (a) The ion distribution functions arising for the sum of two symmetric Maxwellians displaced by  $\pm v_b$  for  $0 < v_b < 2$ . The threshold case is marked in thick black for  $\psi = 0.5$  and thick red for  $\psi = 0.02$ . (b) The force coefficient  $\delta F / \delta x / \psi^2$  as a function of the beam velocity for an equally spaced range of (sech<sup>4</sup> shape) electron hole potential heights  $\psi$ .

Figure 3(a) shows for reference the used sech<sup>4</sup> potential profile including the small shift  $\delta x$  used for calculating  $\delta F$ . Figure 3(b) shows the (unshifted) corresponding first stable density profile (blue) and the adjacent last unstable density profile (green) in which the  $v_b$  is smaller by 0.02. The precise threshold lies between these two  $n(x)$  profiles, corresponding to a density that is nearly flat (but not exactly because of profile and nonlinear effects). Figure 3(c) shows the same thing for a much larger potential peak  $\psi = 0.5$ . One can see that near threshold  $dn(\phi)/d\phi$  actually reverses its sign at large  $\phi$ .

#### D. Positive potential structures sustained by ions?

Since within a local  $f_\infty(v)$  minimum a positive potential gives positive ion charge, one might wonder whether such an effect can by itself be responsible for sustaining the structure. In multiple-humped ion distributions is there such a thing as a slow positive ion soliton? The answer appears to be no. The reason is not stability, but equilibrium. To generate a solitary positive potential peak requires the electric charge to be positive near the peak but negative in the wings. Yes, ion charge perturbation can be positive for positive potential whose velocity lies within a local minimum of the distribution function; but if so, then it is never negative, because actually  $dn/d\phi$  decreases with increasing  $\phi$ . That rules out the required transition from negative to positive ion charge perturbation as  $\phi$  rises moving from the hole wing to the potential peak. Therefore certainly ions alone cannot sustain a slow positive soliton. This contrasts with negative potential *ion holes*, which can be sustained by a deficit of trapped ions.

A Maxwellian electron distribution with no trapped deficit gives a negative charge density perturbation approximately linear with potential ( $\sim -\phi$ ) (see, e.g., Ref. [5]). Electrons therefore *can* give the required negative charge density in the

wings of the hypothesized solitary structure, and do so for a classic ion-acoustic soliton. But to obtain positive charge density near the potential peak, the rise in ion density (in a soliton) has to overwhelm the rise in electron density in the center but not in the wings. That requires the ion density to have substantial positive curvature  $d^2n/d\phi^2$ . It has for a passing ion beam, but it generally does not for a slow structure, because of ion reflection. In fact [compare Fig. 3(c)] at potentials comparable to the width of the  $f(v)$  minimum,  $n(\phi)$  has substantial *negative* curvature (with  $dn/d\phi$  eventually becoming negative). This appears to be a general rule arising from the reflection of progressively higher  $f_\infty(v)$  values as the reflection velocity range expands from a zero lying in a distribution minimum, as required for velocity stability.

Therefore essentially any positive solitary structure that is slow in the sense of having velocity coinciding with the dominant parts of the ion distribution cannot be sustained by ions alone, and cannot be sustained at all unless the electron distribution changes make major contributions to the central positive charge. This restriction is not exactly a watertight proof that positive slow solitary structures are electron holes, but it closes off most plausible alternative possibilities.

### III. ASYMMETRIC DISTRIBUTION FUNCTIONS

Now we must tackle asymmetric ion velocity distributions and their complications.

#### A. Calculation of density

First, if  $f_\infty$  is asymmetric in the incoming sign ( $\sigma_{v_\infty}$  say) of  $v_\infty$ , then the ion density will be a function of *both* the magnitude of the potential *and* the side of potential peak at which the potential occurs. That is because slow ions will be reflected and hence contribute only on one side or the other

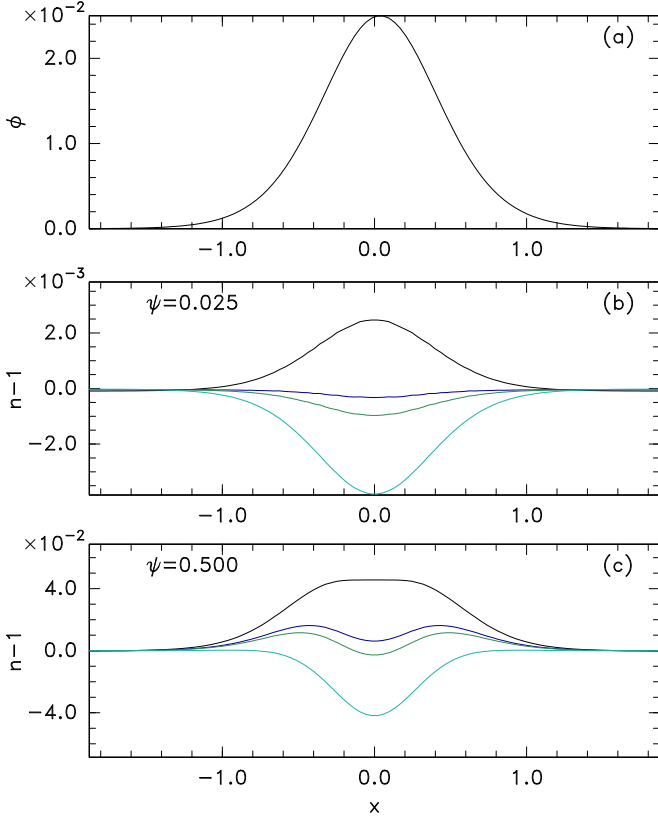


FIG. 3. (a) Slightly shifted  $\text{sech}^4$  potential profile to calculate  $\delta F$ . (b) Ion density as a function of position for the first stable (dark blue) and last unstable (green) velocity shift  $v_b$ , for peak potential  $\psi = 0.5$ , together with cases more stable (black greater  $v_b$ ) and more unstable (light blue smaller  $v_b$ ). (c) Ion density threshold cases like (b) but for greater  $\psi$ .

of the peak (positions  $x$  having sign  $\sigma_x = -\sigma_{v_\infty}$ ). We should therefore refer to the potential in a way that indicates the sign; one convenient way to do so is to express it as the distant incoming velocity that reflects at  $\phi$ :  $v_\phi \equiv -\sigma_x \sqrt{2(\phi - \phi_\infty)} = \sigma_{v_\infty} \sqrt{2(\phi - \phi_\infty)}$ .

But, second, even with this clarification, the density is actually a function of the local potential (and hence  $v_\phi$ ) and

also the height of the potential peak  $\psi$ ; because although in a collisionless situation  $f$  and energy are constant, whether the distribution of particles  $f(x, v)$  moving away from the peak is representative of  $v_\infty$  positive or negative depends on whether those particles have been reflected or have passed over the peak.

So at potential  $\phi$  whose position sign is given by  $-v_\phi$ , the exiting particles ( $v$  and  $x$  having the same sign) have  $f_\infty(v_\infty)$  corresponding to a sign of  $v_\infty$  equal to  $\mp \sigma_x$ , depending on whether they have been reflected or not. That is, for  $v^2/2 + \phi > \psi$  (passing particles),  $f(x, \sigma_x |v|) = f_\infty(-\sigma_x \infty, \sigma_x \sqrt{v^2 + 2[\phi - \phi_\infty]})$ , while for  $v^2/2 + \phi < \psi$  (reflected particles),  $f(x, \sigma_x |v|) = f_\infty(\sigma_x \infty, -\sigma_x \sqrt{v^2 + 2[\phi - \phi_\infty]})$ . Since I find this distinction requires considerable care, I illustrate it graphically in Fig. 4, denoting  $v_\psi = \sqrt{2(\psi - \phi_\infty)}$  (positive value). The  $v_\infty$  ranges that contribute to the density locally at  $\phi(x) = \phi$  for the two signs  $\sigma_{v_\infty} = +1$  ( $\sigma_x = -1$ ) blue, and  $\sigma_{v_\infty} = -1$  ( $\sigma_x = +1$ ) red are shown as horizontal dash-dot lines. A purely illustrative Maxwellian  $f_\infty$  is shown emphasizing that even a shift of a symmetric Maxwellian from the structure velocity (zero) gives rise to asymmetry, and hence dependence of density on  $\psi$ .

The density is given as before by

$$\int f(v) |dv| = \int f_\infty \frac{|v_\infty|}{|v|} |dv_\infty| = \int f_\infty \frac{|v_\infty|}{\sqrt{v_\infty^2 - v_\phi^2}} |dv_\infty|, \quad (11)$$

using  $v dv = v_\infty dv_\infty$  and  $v_\phi^2 \equiv 2(\phi - \phi_\infty)$ , but the tricky part is the three subranges of integration. They give density contributions we may denote  $n_r$  from particles that will be or have been reflected giving two contributions from velocity in  $[v_\phi, \sigma_{v_\infty} v_\psi] = [v_\phi, -\sigma_x v_\psi]$ ,  $n_t$  from particles that have been transmitted  $[\sigma_x v_\psi, \sigma_x \infty]$ , and  $n_u$  (unreflected) from particles that will not be reflected  $[-\sigma_x v_\psi, -\sigma_x \infty]$ :

$$n = n_r + n_t + n_u = \left[ 2 \int_{v_\phi}^{-\sigma_x v_\psi} + \int_{\sigma_x v_\psi}^{\sigma_x \infty} + \int_{-\sigma_x v_\psi}^{-\sigma_x \infty} \right] \times f_\infty \frac{|v_\infty|}{\sqrt{v_\infty^2 - v_\phi^2}} |dv_\infty|. \quad (12)$$

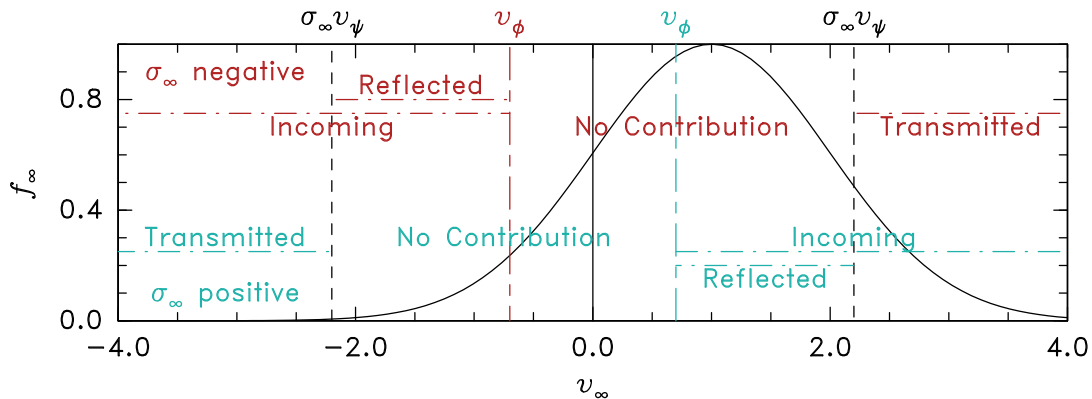


FIG. 4. Distant velocity ranges ( $v_\infty$ , horizontal dash-dot lines) that contribute to the integrals of  $f_\infty(v_\infty)$  giving density, at the two sides of a potential peak:  $\sigma_{v_\infty} = +1$  ( $x$  negative) blue, and  $\sigma_{v_\infty} = -1$  ( $x$  positive) red. Vertical lines at  $v_\phi$  indicate the  $v_\infty$  that reflects at potential  $\phi$  and  $v_\psi$  that reflects at  $\psi$ .

Since each integration range is increasing in absolute value, the sign of  $dv_\infty$  is the same as the sign of  $v_\infty$ ; so  $|v_\infty| |dv_\infty| = v_\infty dv_\infty$  and we need not take moduli. For numerical evaluation it is advantageous as before [Eq. (2)] to integrate by parts to remove the singularity at  $v_\infty^2 = v_\phi^2$ , giving

$$n = [f_\infty(-\sigma_x v_\psi) - f_\infty(\sigma_x v_\psi)] \sqrt{v_\psi^2 - v_\phi^2} - \left[ 2 \int_{v_\phi}^{-\sigma_x v_\psi} + \int_{\sigma_x v_\psi}^{\sigma_x \infty} + \int_{-\sigma_x v_\psi}^{-\sigma_x \infty} \right] f'_\infty \sqrt{v_\infty^2 - v_\phi^2} dv_\infty, \quad (13)$$

in which the integrated parts no longer cancel.

This expression allows us to calculate the density arising everywhere on a potential structure stationary in some inertial frame and the resulting force on the ions  $F = -\int_{-\infty}^{\infty} n(x) \frac{d\phi}{dx} dx = \sum_{\sigma_x = \pm 1} \int_{\phi_\infty}^{\psi} n(\phi, \sigma_x) \sigma_x d\phi$ . However, unlike the symmetric case, no symmetry now tells us what the equilibrium velocity of that frame relative to the ion distribution should be. And for an arbitrary frame velocity  $v_h$  relative to the ion distribution, there will generally be a nonzero ion force  $F(v_h)$ . Then the configuration will not be in equilibrium because the structure potential will be subject to a net force  $-F$ . Only for the particular structure velocity that makes  $F(v_h) = 0$  will there be an equilibrium. (This is true also for a distribution like a sum of two similar but shifted Maxwellians, that has velocity symmetry in *some other* frame of reference; but we previously tacitly adopted that particular frame of reference as our equilibrium structure frame.)

### B. Velocity equilibrium and stability

For  $f_\infty$  intrinsically asymmetric we need to find both the equilibrium electron hole velocity (potential structure velocity),  $v_{h0}$ , and the derivative of the force with respect to a shift of the structure relative to its equilibrium position,  $\delta F/\delta x$ , to determine the equilibrium's stability to rapid motion of the potential structure leaving behind a fixed ion density. However before we do that, a second factor concerning stability arises in respect of  $dF/dv_h$ . If we find an equilibrium hole velocity, which has  $F = 0$ , then how does  $F$  vary when we consider a neighboring hole *velocity* (not *position*)? This question governs the stability of the situation for slow hole acceleration in the opposite limit where the ion density perturbation accelerates with the potential structure. If  $F$  changes in such a direction as to oppose the acceleration, then the equilibrium is stable to such acceleration; but if not, then the equilibrium is unstable. Of course, in reality the two types of hole motion, having stationary ion density, or having perfectly tracking ion density, are approximate extreme limits of a continuous response dependent on frequency. Full frequency analysis proves to be mathematically challenging even for an ion stream that is well separated from the hole velocity, but has been completed showing oscillatory instability for hole speed down to a few ion sound speeds [9]. In the present work we content ourselves instead with the combination of a more heuristic pair of approximations: the extreme limits of fast and slow. This renders stability criteria but not precise eigenvalues.

We can formulate a lumped parameter treatment by supposing that we can combine the two different perturbations of the ion force arising from the coefficients  $\delta F/\delta x$  and  $dF/dv_h = dF/d\dot{x}$  into a second order system:  $M\dot{v}_h = M\ddot{x} = -(\delta F/\delta x)x - (dF/d\dot{x})\dot{x}$ , (recalling that  $F$  is the force on the particles, which is minus the force on the hole). It has the form

$$\ddot{x} + \frac{dF}{Mdx}\dot{x} + \frac{\delta F}{M\delta x}x = \ddot{x} + b\dot{x} + cx = 0. \quad (14)$$

The solutions of this linear second-order equation are stable if and only if both  $c$  and  $b$  are non-negative. In that case, it is a damped harmonic oscillator equation. When instead  $c$  is negative, then an exponentially growing solution dominates the long-time behavior. If  $c$  is positive but  $b$  is negative, then a growing oscillation is the instability. Stability of the electron hole requires both  $c = C/M = \frac{\delta F}{M\delta x}$  and  $b = \frac{dF}{Md v_h}$  to be positive. And since  $M$  is negative that means the two ion force derivatives must be negative.

Finding a stable equilibrium is carried out as follows. For a given distribution, the structure velocity  $v_h$  is scanned in small steps relative to the ion distribution to find the first (and usually the only) value at which the force  $F$  changes from positive to negative ( $dF/dv_h < 0$ , making  $b$  positive) and also the value of  $\delta F/\delta x$  is negative so  $c$  is positive (i.e., stable). If no such  $v_h$  is found, then the distribution does not permit stable slow electron holes.

The other major approximation we make here is that we do not calculate self-consistently the form of the electron hole potential  $\phi(x)$ . For symmetric distributions, in principle we could choose it to be whatever we like and find the required self-consistent trapped electron distribution through the integral equation analysis of Bernstein, Greene, and Kruskal [5,6]. Since here we are calculating the effects on a known potential of the interaction with the ions, it is sufficient just to prescribe the potential, especially since as noted in Sec. II C the detailed shape of the potential has only a rather weak effect. However, for asymmetric ion distributions and finite hole peak potential  $\psi$ , it is no longer the case that the ion density is the same on the two sides of the electron hole. Therefore it is far from obvious that the potential need be the same on the two sides either. When it is not and  $\phi_\infty$  is different for  $\pm\sigma_x$ , the potential structure has the form of a nonmonotonic double layer [30] and many additional complexities arise, which it is not the purpose to address here. Therefore we continue by setting aside these complications, assuming a symmetric potential form  $\phi(x) \propto \text{sech}^4 x$  and limiting the applicability of the present result to electron holes or other structures that have negligible net potential drop across them. Detailed analysis, in preparation for a future publication, shows that this is a good approximation.

The specific distribution shapes considered here are adequately represented by the sum of two Maxwellian components shifted from each other by  $2v_b$ . The widths and relative densities of the two components can be prescribed so as to represent different generic shapes. The shift parameter  $v_b$  determines how deep any local minimum in the distribution is. The threshold value of  $v_b$ , at which stable electron holes become permitted, is found by the following outer iteration of the above described structure velocity  $v_h$  scan. A relatively

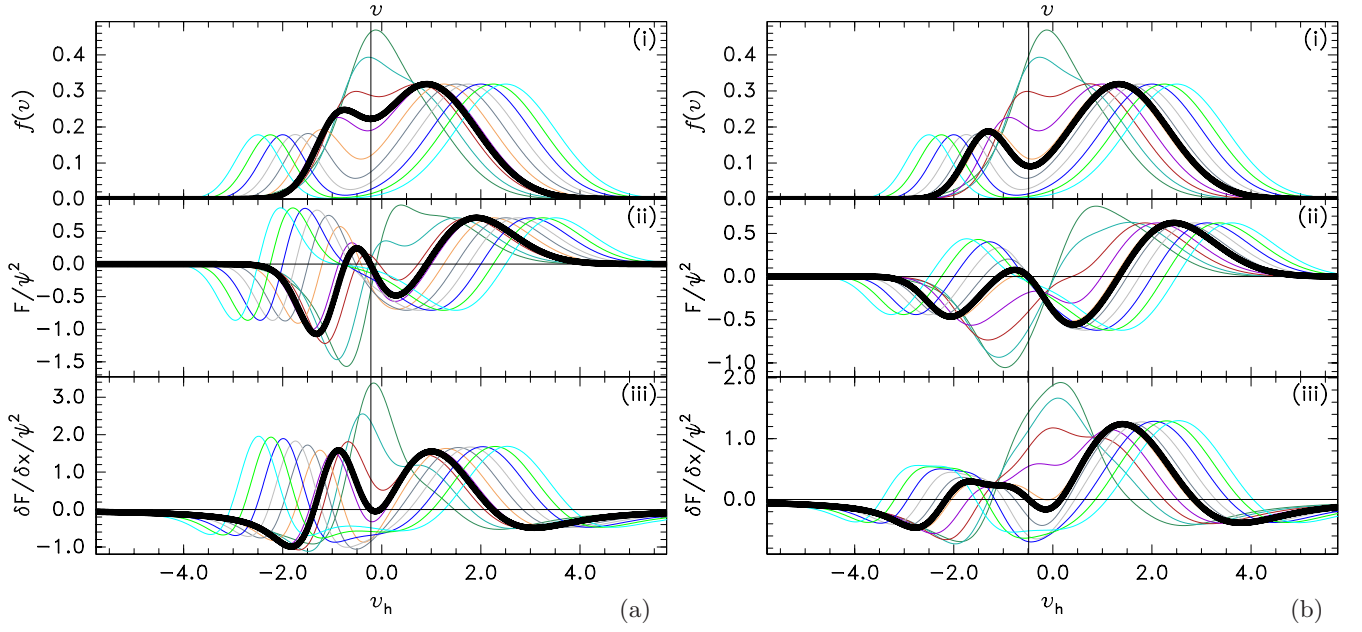


FIG. 5. Distribution function (i)  $f(v)$ , force (ii)  $F(v_h)$ , and stability coefficient (iii)  $\delta F/\delta x$ , as a function of velocity ( $v$  and  $v_h$ ), for a range (different colors) of distribution beam shift parameter  $v_b$ . Thick black line is the threshold case for stable electron hole existence. (a)  $\psi = 0.02$ ; (b)  $\psi = 0.5$ .

coarse  $v_b$  scan is carried out over a range sufficient to cover all desired distributions, and the smallest  $v_b$  that permits a stable equilibrium is found. An example scan is shown by the different colored lines in Fig. 5. The threshold  $v_b$  is then refined by setting the last  $v_b$  that did not permit an equilibrium and the first that did permit it as the lower and upper limits of a new scan of  $v_b$  with the same number of steps (hence much smaller steps). Refined scans are not plotted. This process of decreasing the step size by a factor equal to the number of steps in the scan is iterated; when 10 steps are taken, two more iterations are enough to converge within other uncertainties. The stable case of the final  $v_b$  scan is interpolated for the threshold, and is plotted in thick black. The vertical line indicates the stable structure velocity  $v_{h0}$ .

It is observed in this and all other cases explored that the stable  $v_{h0}$  lies within a distribution function local depression but not necessarily exactly at the velocity of minimum  $f(v)$ . A stable electron hole equilibrium is found only if there exist three stationary points (two maxima and one minimum between them) of  $f(v)$ , and  $v_{h0}$  always lies between the locations of the maxima. It is also found that the required fractional depth of the minimum increases as  $\psi$  is increased, as the comparison between Fig. 5(a) and Fig. 5(b) illustrates.

A wider-ranging graphical impression of the range of marginal distribution shapes is given by Fig. 6. Each frame shows marginally stable distributions for  $\psi = 0.05$  (green) and  $\psi = 0.5$  (blue), for different temperature  $T_2$  and fractional density  $n_2$  of the second Maxwellian component (toward negative  $v$ ). The first component has  $T_1 = 1$  and  $n_1 = 1 - n_2$ . The equilibrium hole velocity  $v_{h0}$  is shown by the cross.

An estimate of the size of the damping coefficient  $b$  can be obtained by the observation that the typical value of  $dF/dv_h$  in plots like Fig. 5 is of order  $-0.5\psi^2$  or smaller. Since the dimensionless hole mass is  $M = -(m_e T_0/m_i T_e) \int \phi dx =$

$-(m_e T_0/m_i T_e)L\psi$  and typically  $L = (16/3)\sqrt{T_e/T_0}$  we have

$$|b| = \left| \frac{dF}{M dv_h} \right| \lesssim 0.1 \frac{m_i}{m_e} \sqrt{\frac{T_e}{T_0}} \psi. \quad (15)$$

This is rather comparable to the maximum absolute value of  $c$  in ion dimensionless units,

$$|c| = \left| \frac{\delta F}{M \delta x} \right| \lesssim \left( \frac{3}{16} \right)^2 \frac{m_i}{m_e} \psi, \quad (16)$$

for  $\sqrt{T_e/T_0}$  not much different from unity. The large values of both would mean that harmonic solutions would in fact be more than critically damped. However, since the resulting timescales are very short compared with  $1/\omega_{pi}$ , the mechanism of the ion density perturbation perfectly changing with hole motion as if in steady state, giving rise to (b), is liable to be a very poor quantitative approximation, unlike the stationary ion mechanism (c) which is the opposite extreme. Nevertheless, the fact of  $b$ 's sign being that of damping is an important indication that slow hole motions with  $c$  near zero will in fact be stable. A proper treatment for arbitrary frequency, of course, requires solution of the time-dependent Vlasov equation for ions, which is not attempted here.

#### IV. ION DISTRIBUTION LINEAR STABILITY

The background one-dimensional warm two-beam ion distributions might experience sinusoidal linear electrostatic instability not caused by solitary structures, depending on the spacing, relative density, and velocity-width of the beams, and on the electron temperature [31,32]. Generally this ion-ion instability requires a local minimum in the ion distribution of a certain depth. It is conceivable that such an instability might contribute to the mechanism that forms an electron hole, but that is not the focus here. However, the question arises



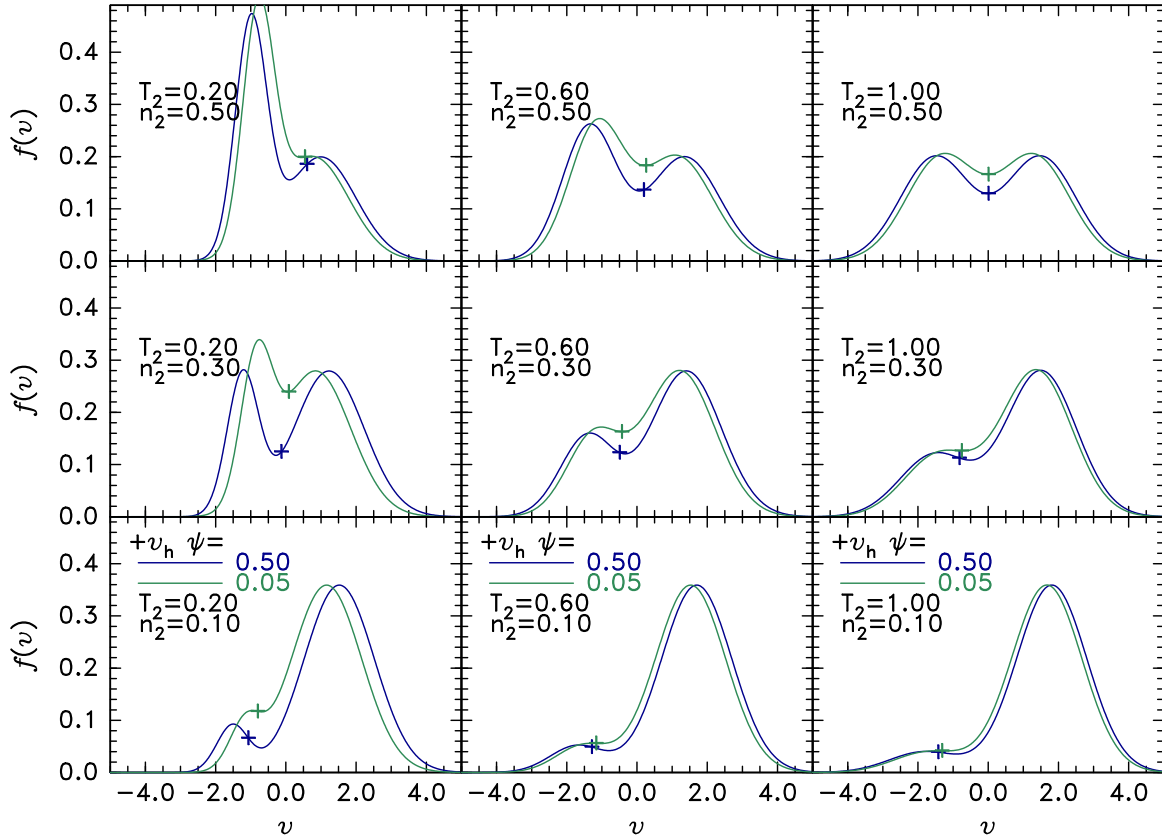


FIG. 6. A range of marginal ion distribution shapes for two-Maxwellian distributions.

as to whether the non-single-humped background plasma ion distribution *required for persistence* of slow electron holes is stable to ion-ion modes. If not, then perhaps electron hole existence would be prevented because the required background distribution minimum is unstable. The ion-ion instability can be explained in outline, with reference to Fig. 7, obtained by a numerical method of analyzing and visualizing these and other kinetic ion instabilities for arbitrary ion distributions developed by the present author, mostly for pedagogic purposes (see Ref. [33]).

The one-dimensional ion velocity distribution being analysed is shown in the upper panel. The small middle panel shows the peak of the electron distribution function with temperature  $T_e = T_0$ , to indicate its very different velocity scale and the limited extent to which its gradient is significant.

For a wave of complex frequency  $\omega$ , real wave number  $k$ , and thus phase velocity  $v_p = \omega/k$  the lower panel shows contours on the complex phase velocity plane (scaled to an ion speed  $\sqrt{T_0/m_i}$  where  $T_0$  is a reference temperature) of the complex quantity  $(k\lambda_D)^2\chi_i$ ; the Debye length is  $\lambda_D = \sqrt{\epsilon_0 T_0/e^2 n_e}$ , and  $\chi_i$  is the ion susceptibility. For species  $j$ , the quantity

$$k^2\lambda_D^2\chi_j = -(\lambda_D\omega_{pj})^2 \int \frac{\partial f_j}{\partial v} \frac{1}{v - v_p} dv, \quad (17)$$

(integrating along the Landau contour) is a function only of the ion distribution shape and (complex)  $v_p$ , not of  $\omega$  and  $k$  separately. The dispersion relation for electrostatic waves is  $\chi = \chi_e + \chi_i = -1$ . Therefore any solution must have the

imaginary part of  $\chi$  equal to zero. Contours of zero imaginary part of  $\chi_i$  and of  $\chi$  are shown in black and blue respectively. The electron susceptibility (for Maxwellian electron temperature  $T_e$ ) gives to an excellent approximation  $(k\lambda_D)^2\chi_e = (T_0/T_e)(1 + iv_p\sqrt{\pi m_e/2T_e})$ , and contributes an adjustment to the imaginary part of  $\chi$  at large  $|\text{Re}(v_p)|$ , which is electron Landau damping of ion-acoustic waves. But for the low velocity instability this contribution is negligible and the black and blue contours coincide.

The electron contribution to the real part of  $(k\lambda_D)^2\chi$  is to an excellent approximation simply  $(T_0/T_e)$ . And the real part of the dispersion relation is then  $k^2\lambda_D^2 = -\text{Re}(k^2\lambda_D^2\chi_i) - T_0/T_e$ ; so the intersection of the zero imaginary contour with a green contour indicates the value of dispersion solution's wave number. If  $k$  is regarded as a free choice, then the dispersion relation can be satisfied for some  $k$  if  $\text{Re}(k^2\lambda_D^2\chi_i) + T_0/T_e$  is negative. Therefore the limiting solution of the dispersion relation as  $k \rightarrow 0$  lies at  $\text{Re}(k^2\lambda_D^2\chi_i) = -T_0/T_e$ , and when  $T_e/T_0 \rightarrow \infty$  it is at  $\text{Re}(k^2\lambda_D^2\chi_i) = 0$ . Where the appropriate contour of  $\text{Re}(k^2\lambda_D^2\chi_i)$  crosses the zero contour of  $\text{Im}(\chi)$  is the dispersion solution for  $v_p$ . If the intersection lies below the real axis, then the mode is damped; if above, then it is growing (unstable). In regions where  $\text{Re}(k^2\lambda_D^2\chi_i)$  is positive, no solutions exist (regardless of non-negative electron temperature) and the plane is shaded dark gray. In regions where  $\text{Re}(k^2\lambda_D^2\chi_i) > -1$  no solution exists for  $T_e \leq T_0$ , and the regions where it lies between  $-1$  and  $0$  are shaded light gray. The green contours for different negative values  $-(0, 2, 5, 1, 2, 5, 10)$  of  $\text{Re}(k^2\lambda_D^2\chi_i)$  therefore correspond to boundaries of solution regions for  $T_e = -T_0/\text{Re}(k^2\lambda_D^2\chi_i)$ .

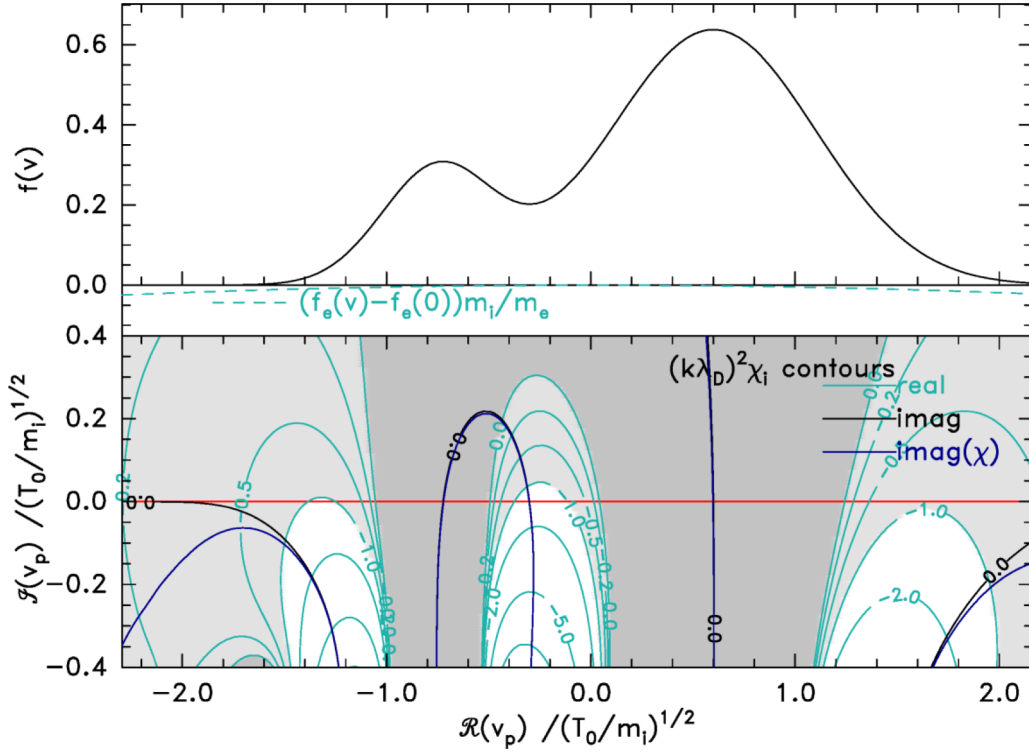


FIG. 7. Contours of scaled susceptibility on the complex phase velocity plane. Dispersion relation solutions lie at intersections of the black or blue contours with the green contours. No solutions exist in dark shaded regions. Solutions exist in light shaded regions only for  $T_e \geq T_0$ .

Two-beam distributions like Fig. 7 have three unshaded regions where solutions exist. Those on the right and left are the positively and negatively propagating ion-acoustic waves, lying below the real axis when electron Landau damping is included. The central region coinciding with the distribution local minimum is where ion-ion instability solutions lie. The stability of this ion-ion mode is not significantly influenced by electron Landau damping. Changing the electron temperature changes the stability not by changing the local electron distribution *gradient* but by changing its *height* (inversely with its overall width).

There is therefore a threshold electron temperature above which a (sufficiently) double-humped ion distribution becomes unstable. This temperature is a convenient way to parametrize the ion-ion stability of the distribution, and it can be found simply by examining  $k^2 \lambda_D^2 \chi_i$  along the real  $v_p$  axis, and finding its real value at the velocity where its imaginary part is zero, giving  $T_{\text{threshold}} = -T_0 / \text{Re}(k^2 \lambda_D^2 \chi_i)$ . This is equivalent to the standard Nyquist stability analysis used in this context by Penrose [34] but expressed in a different way.

Figure 8 shows contours of  $T_{\text{threshold}}$  as a function of the distribution parameters. Those parameters are ordered like Fig. 6, which therefore shows qualitatively how the distribution shape changes over the contour plane. Higher  $T_{\text{threshold}}$  are more stable cases. The first component of the two-Maxwellian distribution has temperature  $T_0 = 1$ , and density  $1 - n_2$ , where  $n_2$  is the total density of the second component, whose temperature is  $T_2$ . Thus  $n_2$  and  $T_2$  together determine the shape of the distribution, because the component velocity separation  $2|v_b|$  is found by the process described in Sec. III B. In other words  $|v_b|$  is taken to be the minimum that allows the

persistence of an electron hole. *That* beam separation is never large enough that the purely one-dimensional ion-ion mode is more stable than the obliquely propagating mode (which can happen for large  $|v_b|$  [35]); so if the ion distribution is stable by the one-dimensional analysis, then it is stable to all unmagnetized electrostatic ion-ion modes.

Figure 8(a) is for a large amplitude hole  $\psi = 0.5$  which requires substantially deeper minimum in the distribution (larger  $|v_b|$  and hence less stable) than Fig. 8(b). The value  $\psi = 0.1$  (b) is representative of small  $\psi$ . The uncertainty level of perhaps a few percent in the threshold away from the sharp cliff probably arises from the discrete velocity meshes and from the relatively coarse parameter mesh  $20 \times 20$ . Since large  $T_{\text{threshold}}$  occurs for some regions, contours are not shown above  $T_{\text{threshold}} = 10$  (a) or 20 (b).

At the rather large (and hence more unstable) amplitude  $\psi = 0.5$  (a), even for unusually small  $T_2$  no ion-ion instability occurs until  $T_e \gtrsim T_0$  or in fact  $T_e \gtrsim 6T_{\text{min}}$ , where  $T_{\text{min}}$  is the smaller of the two components' ion temperatures, no matter what  $n_2$  is. For small amplitude holes ( $\psi = 0.1$ ) (b),  $T_{\text{threshold}} \gtrsim 20T_{\text{min}}$  over the great majority of the plane, showing that the marginal distribution for the existence of small amplitude holes is highly stable to the ion-ion mode.

## V. CONCLUSIONS

Long-lived one-dimensionally stable slow electron hole equilibria can exist only when the background ion velocity distribution has a sufficiently deep local minimum and the electron hole speed lies within it. If the electron tempera-

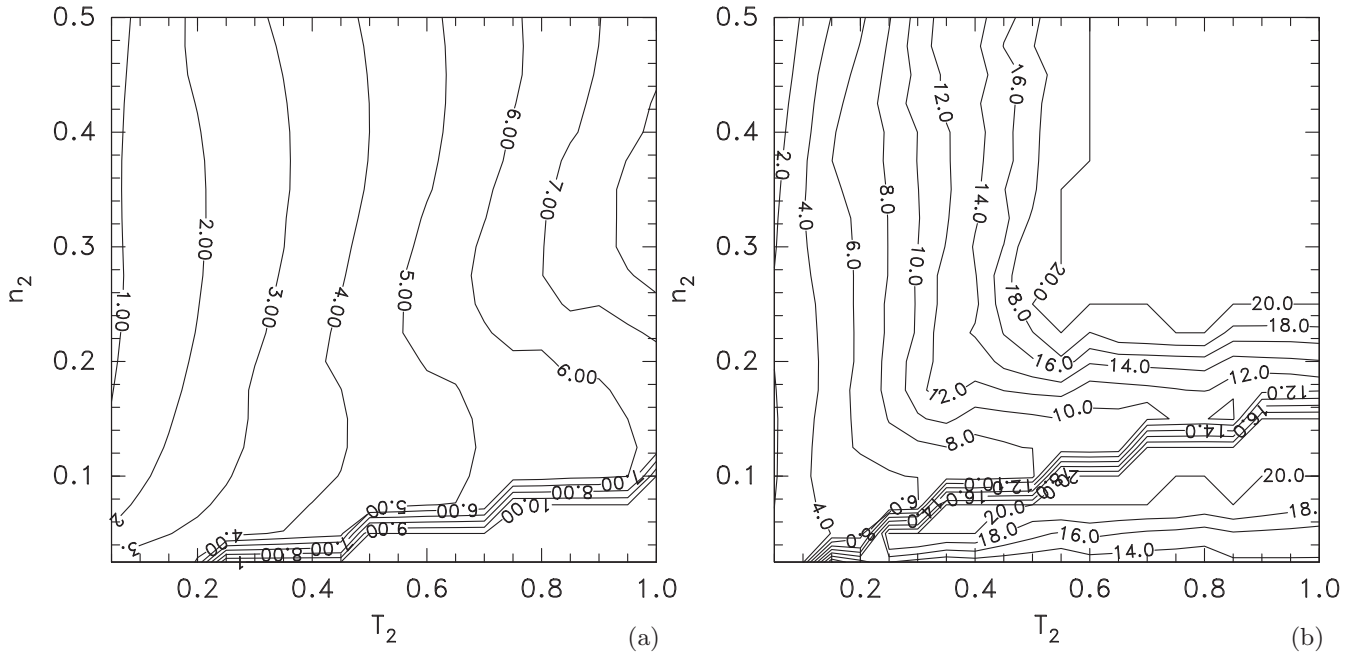


FIG. 8. Contours of the electron temperature  $T_{\text{threshold}}$  above which ion-ion instability occurs in two-Maxwellian distributions for which the first component has unit temperature and the second component temperature  $T_2$  and fractional density  $n_2$ , and the shift between them is minimal for the existence of electron holes having (a)  $\psi = 0.5$  and (b)  $\psi = 0.1$ .

ture is less than  $\sim 6$  to 20 times the effective temperature of the colder ion component, then the required background ion distribution will be linearly stable; so there is no (linear electrostatic, one-dimensional) stability reason it should not exist. The ion density change caused by a solitary positive potential peak whose velocity lies in the local minimum, is positive, avoiding the self-acceleration of the hole that otherwise occurs. However, ion charge perturbations alone cannot create the conditions for a *slow* positive soliton, and the electron charge perturbation of a distribution without phase-space-density deficit in the trapped region cannot permit a total charge density positive at the potential peak and negative in the wings, as is required for a soliton. Therefore it seems that persistent, slow, positive, solitary potential structures must be sustained primarily by trapped electron deficit. That is, they must be electron holes. And their velocity must lie within a local minimum in the ion velocity distribution. It is not impossible that slow electron holes might be observed as they form, or shortly afterwards, in ion distributions that do not possess the local minimum found here. But they would be

expected to be unstable, and so rapidly be self-accelerated to speeds that are no longer slow.

All of the analysis presented here is purely one-dimensional. However, it seems possible that the ion coupling effects explored might also have a significant effect on the multidimensional transverse stability of electron holes, by altering the force-balance that determines it [36]. If so, which is a possible topic for future analysis, then they might have different typical transverse sizes than fast electron holes or even persist at lower magnetic field strengths.

#### ACKNOWLEDGMENTS

I am grateful to I. Y. Vasko, Y. Kamaletdinov, and A. V. Artemyev for stimulating discussions of slow electron holes, especially their recent analysis of MMS observations confirming that they lie in minima of  $f_i(v)$ . The present work was not supported by any external public funding. The code used to calculate and plot the figures is in Ref. [37]; no data were used.

- [1] D. B. Graham, Y. V. Khotyaintsev, A. Vaivads, and M. André, Electrostatic solitary waves and electrostatic waves at the magnetopause, *J. Geophys. Res.: Space Phys.* **121**, 3069 (2016).
- [2] K. Steinvall, Y. V. Khotyaintsev, D. B. Graham, A. Vaivads, P.-A. Lindqvist, C. T. Russell, and J. L. Burch, Multispacecraft analysis of electron holes, *Geophys. Res. Lett.* **46**, 55 (2019).
- [3] A. Lotekar, I. Y. Vasko, F. S. Mozer, I. Hutchinson, A. V. Artemyev, S. D. Bale, J. W. Bonnell, R. Ergun, B. Giles, Y. V. Khotyaintsev, P.-A. Lindqvist, C. T. Russell, and R. Strangeway, Multisatellite mms analysis of electron holes in

the earth's magnetotail: Origin, properties, velocity gap, and transverse instability, *J. Geophys. Res.: Space Phys.* **125**, e2020JA028066 (2020).

- [4] H. Schamel, Electrostatic phase space structures in theory and experiment, *Phys. Rep.* **140**, 161 (1986).
- [5] I. H. Hutchinson, Electron holes in phase space: What they are and why they matter, *Phys. Plasmas* **24**, 055601 (2017).
- [6] I. B. Bernstein, J. M. Greene, and M. D. Kruskal, Exact nonlinear plasma oscillations, *Phys. Rev.* **108**, 546 (1957).

- [7] I. H. Hutchinson and C. Zhou, Plasma electron hole kinematics. I. Momentum conservation, *Phys. Plasmas* **23**, 82101 (2016).
- [8] C. Zhou and I. H. Hutchinson, Plasma electron hole kinematics. II. Hole tracking Particle-In-Cell simulation, *Phys. Plasmas* **23**, 82102 (2016).
- [9] C. Zhou and I. H. Hutchinson, Plasma electron hole ion-acoustic instability, *J. Plasma Phys.* **83**, 90580501 (2017).
- [10] R. C. Davidson, *Methods in Nonlinear Plasma Theory* (Academic Press, New York, 1972).
- [11] K. Saeki and J. J. Rasmussen, Stationary solution of coupled electron hole and ion soliton in a collisionless plasma, *J. Phys. Soc. Jpn.* **60**, 735 (1991).
- [12] K. Saeki and H. Genma, Electron-Hole Disruption Due to Ion Motion and Formation of Coupled Electron Hole and Ion-Acoustic Soliton in a Plasma, *Phys. Rev. Lett.* **80**, 1224 (1998).
- [13] C. Zhou and I. H. Hutchinson, Dynamics of a slow electron hole coupled to an ion-acoustic soliton, *Phys. Plasmas* **25**, 082303 (2018).
- [14] C. Norgren, M. André, D. B. Graham, Y. V. Khotyaintsev, and A. Vaivads, Slow electron holes in multicomponent plasmas, *Geophys. Res. Lett.* **42**, 7264 (2015).
- [15] C. Norgren, M. André, A. Vaivads, and Y. V. Khotyaintsev, Slow electron phase space holes: Magnetotail observations, *Geophys. Res. Lett.* **42**, 1654 (2015).
- [16] J. F. Drake, M. Swisdak, C. Cattell, M. A. Shay, B. N. Rogers, and A. Zeiler, Formation of electron holes and particle energization during magnetic reconnection, *Science (New York, NY)* **299**, 873 (2003).
- [17] Y. V. Khotyaintsev, A. Vaivads, M. André, M. Fujimoto, A. Retinò, and C. J. Owen, Observations of Slow Electron Holes at a Magnetic Reconnection Site, *Phys. Rev. Lett.* **105**, 165002 (2010).
- [18] L. Muschietti, I. Roth, R. E. Ergun, and C. W. Carlson, Analysis and simulation of BGK electron holes, *Nonlin. Process. Geophys.* **6**, 211 (1999).
- [19] B. Eliasson and P. K. Shukla, Dynamics of Electron Holes in an Electron-Oxygen-Ion Plasma, *Phys. Rev. Lett.* **93**, 045001 (2004).
- [20] B. Eliasson and P. K. Shukla, Formation and dynamics of coherent structures involving phase-space vortices in plasmas, *Phys. Rep.* **422**, 225 (2006).
- [21] C. B. Haakonsen, I. H. Hutchinson, and C. Zhou, Kinetic electron and ion instability of the lunar wake simulated at physical mass ratio, *Phys. Plasmas* **22**, 32311 (2015).
- [22] A. Kakad, B. Kakad, C. Anekallu, G. Lakhina, Y. Omura, and A. Fazakerley, Slow electrostatic solitary waves in earth's plasma sheet boundary layer, *J. Geophys. Res.: Space Phys.* **121**, 4452 (2016).
- [23] T. H. Dupree, Theory of phase-space density holes, *Phys. Fluids* **25**, 277 (1982).
- [24] S. R. Kamaletdinov, I. H. Hutchinson, I. Y. Vasko, A. V. Artemyev, A. Lotekar, and F. Mozer, Spacecraft observations and theoretical understanding of slow electron holes (unpublished).
- [25] A recent paper [26] reports Vlasov simulations appearing to show for Maxwellian distributions at  $T_i/T_e = 10$  that self-acceleration is suppressed. It claims that high-enough ion temperature  $T_i/T_e > 3.5$  can reverse the ion density response. That claim is proven by the present simple derivation to be incorrect. The simulation code is not initialized self-consistently, resulting in potential oscillations much larger than the extremely small hole potential; these factors cast doubt on its results, which contradict several other code simulations at larger amplitude. The analysis included to explain its results is faulty.
- [26] D. Mandal, D. Sharma, and H. Schamel, Ultra slow electron holes in collisionless plasmas: Stability at high ion temperature, *Phys. Plasmas* **27**, 022102 (2020).
- [27] A pure shift of the potential structure is justified if the ion charge contribution to the equilibrium hole is small compared with the electron. If not, then the magnitude of the force increment will be only approximate; nevertheless, its sign, which determines stability, will not be changed.
- [28] T. H. Dupree, Growth of phase-space density holes, *Phys. Fluids* **26**, 2460 (1983).
- [29] Strictly, Eq. (7) applies when ion charge response is neglected. That neglect is not immediately obvious for slow holes. However, at the threshold of instability the ion charge response actually *is* negligible, so it is appropriate to invoke the equation for thresholds. When estimates of unstable positive growth rate  $\gamma \neq 0$  are later obtained from it, one should beware of the approximation and take these as approximate only.
- [30] M. A. Raadu, The physics of double layers and their role in astrophysics, *Phys. Rep.* **178**, 25 (1989).
- [31] T. E. Stringer, Electrostatic instabilities in current-carrying and counterstreaming plasmas, *J. Nucl. Energy C: Plasma Phys.* **6**, 267 (1964).
- [32] B. D. Fried and A. Y. Wong, Stability limits for longitudinal waves in ion beam plasma interaction, *Phys. Fluids (1958–1988)* **9**, 1084 (1966).
- [33] <https://github.com/ihutch/chiofv>.
- [34] O. Penrose, Electrostatic instabilities of a uniform non-Maxwellian plasma, *Phys. Fluids* **3**, 258 (1960).
- [35] D. W. Forslund and C. R. Shonk, Numerical Simulation of Electrostatic Counterstreaming Instabilities in Ion Beams, *Phys. Rev. Lett.* **25**, 281 (1970).
- [36] I. H. Hutchinson, Transverse instability magnetic field thresholds of electron phase-space holes, *Phys. Rev. E* **99**, 053209 (2019).
- [37] <https://github.com/ihutch/slowholes>.